Available online at www.sciencedirect.com
ScienceDirect
Trans. Nonferrous Met. Soc. China 25(2015) 713−720
Transactions of Nonferrous Metals Society of China
www.tnmsc.cn

Influence of *I*-phase and *W*-phase on microstructure and mechanical properties of Mg−8Li−3Zn alloy

Guo-bing WEI[1], Xiao-dong PENG[1,2], Bao ZHANG[1], Amir HADADZADEH[3], Tian-cai XU[1], Wei-dong XIE[1,2]

1. College of Materials Science and Engineering, Chongqing University, Chongqing 400044, China;
2. National Engineering Research Center for Magnesium Alloys, Chongqing University, Chongqing 400044, China;
3. Department of Mechanical and Mechatronics Engineering, University of Waterloo, Waterloo ON N2L 3G1, Canada

Received 1 April 2014; accepted 24 July 2014

Abstract: Microstructures and mechanical properties of LZ83−*x*Y alloys containing *I*-phase and *W*-phase were investigated by XRD, OM, SEM and EDS. The experimental results show that the content of *I*-phase and *W*-phase changes by varying Zn/Y mass ratio in the LZ83−*x*Y alloys. The cohesion of *I*-phase/*α*-Mg eutectic pockets can enhance the strength in the as-cast LZ83−0.5Y and LZ83−1.0Y alloys, while the *W*-phase has no obvious strengthening effect on the LZ83−1.5Y alloy. In the extruded alloys, the *I*-phase and *W*-phase were extruded into the particles with nanoscale size in the *β*-Li matrix phase. The dispersion strengthening of *W*-phase was more obvious because of the higher volume fraction. The ultimate tensile strength of extruded LZ83−1.5Y alloy is up to 238 MPa while the elongation is up to 20%.

Key words: Mg−8Li−3Zn alloy; *I*-phase; *W*-phase; mechanical properties; as-cast microstructure

1 Introduction

Mg−Li alloy is one of the lightest and most recyclable structural materials, and it also possesses high specific strength and specific stiffness [1−3]. The density of Mg−Li alloys is about 1.35−1.65 g/cm^3, lower by 1/4 than AZ31 (1.77 g/cm^3) and 1/3 than AZ91 (1.81 g/cm^3) alloys [4,5]. Therefore, the application of Mg−Li alloys in the electrical appliances, automobiles and aerospace vehicles is drawing much attention from the environmental viewpoint [1,6−8].

According to the Mg−Li phase diagram, for Li content less than 5.5%, the Mg−Li alloy is comprised of a single *α*-Mg phase with HCP structure by Li dissolving in Mg. Just like other Mg alloys, the alloys with single HCP structure possess relatively high strength but poor plasticity. While Li content is more than 11.5%, the Mg−Li alloy exclusively consists of the BCC *β*-Li phase. These alloys have excellent formability and extra-low density, but exhibit low mechanical strength and poor corrosion resistance [6,9]. So, they are not applied in the industrial fields widely. Mg−Li alloys exhibit a two-phase microstructure for the 5.5%−11.5% Li content, consisting of *α*-Mg (HCP) and *β*-Li (BCC) phases at room temperature [9]. The existence of *β*-Li phase (BCC crystal structure) makes Mg−Li alloys possess higher elongation than other magnesium alloys. Moreover, the dual-phase Mg−Li alloys usually have better comprehensive mechanical properties than single phase alloys [10].

To further enhance the mechanical properties of Mg−Li alloys, alloying is one of the most commonly used methods. Addition of the most common alloying elements such as Al and Zn can lead to high strength through precipitation strengthening and solution hardening in Mg−Li base alloys [11,12]. The addition of Al to Mg−Li alloys improves the strength, but it causes elongation reduction [6,9]. The addition of Zn has similar effect in Mg−Li base alloys, but the deterioration of elongation is less serious than addition of Al [6]. Magnesium alloys containing rare earth (RE) elements such as yttrium are interesting as light structural material with high strength at both room and elevated temperatures. One possible composition would be an alloy with 8% Li (a mixture of *α*+*β* phases) that might

Foundation item: Project (2007CB613702) supported by the National Basic Research Program of China; Project (CDJZR14130007) supported by the Fundamental Research Funds for the Central Universities, China
Corresponding author: Xiao-dong PENG; Tel: +86-23-65111625; Fax: +86-23-65102602; E-mail: PXD@cqu.edu.cn
DOI: 10.1016/S1003-6326(15)63656-1

exhibit improved mechanical properties. Further improvement of mechanical properties is possible if the alloy is reinforced with zinc and a rare earth element, such as yttrium [10,13].

It has been shown that there are three kinds of ternary equilibrium phases in Mg−Zn−Y system: *W*-phase ($Mg_3Zn_3Y_2$, cubic structure), *I*-phase (Mg_3Zn_6Y, icosahedral quasicrystal structure, quasi-periodically ordered) and *Z*-phase ($Mg_{12}ZnY$, an 18R long period modulated structure) [14,15]. It has been observed that if Zn/Y mass ratio exceeds 4.38:1, the element Y would exist almost completely as *I*-phase [16,17]. The optimum Zn/Y ratio for the formation of two-phase microstructure consisting of *α*-Mg and *I*-phase is 5:1−7:1 in Mg alloys [18]. Previous work indicated that when Zn/Y ratio was lower than 1.10:1, element Y would almost fully exist in the form of *W*-phase [16,17]. When the Zn/Y ratio is between 1.10:1 and 4.38:1, the microstructure includes *I*-phase and *W*-phase simultaneously. Moreover, it has been reported that Mg−Zn−Y alloys containing thermally stable *I*-phase exhibit a significantly high level of yield strength and ductility at the ambient temperature [19]. The strength of Mg−Zn−Y alloys increases with increasing total solute content (Zn and Y), especially with increasing volume fraction of *I*-phase [19,20]. Due to the cubic structure of *W*-phase and the incoherency between *W*-phase and Mg matrix, the atomic bonding between *W*-phase and Mg matrix is very weak [14]. When the volume fraction of *W*-phase reaches 13.8% in as-cast Mg−Zn−Y−Zr alloy, the mechanical properties of the alloy will degrade [20]. Previous work [21] indicated that due to the finer net-like microstructure and the dispersion strengthening effect of *W*-phase after extrusion, the strength can be improved with the increase of *W*-phase. It is well known that during the tensile test, the secondary phases distributed at the grain boundaries can effectively retard the dislocation movement [10]. Though, it has been reported that Mg alloys containing *I*-phase or *W*-phase with a certain value as a secondary solidification phase exhibit good mechanical properties at room temperature as well as elevated temperatures [17,20,22]. However, review of the published literature shows that there is very limited information on the effect of *I*-phase and *W*-phase on the properties of as-cast and extruded Mg−Li alloys.

In the current study, three Mg−Li alloys were designed with different Zn/Y ratios to determine the effect of *I*-phase and *W*-phase on the microstructure and mechanical behavior. As-cast and extruded alloys were studied in terms of microstructural evolution by optical and scanning electron microscope and X-ray diffraction. The mechanical properties were evaluated by the uniaxial tensile test.

2 Experimental

Pure Mg, pure Li, pure Zn and Mg−10Y master alloys were used to prepare the Mg−8Li−3Zn−*x*Y (LZ83−*x*Y) (*x*=0, 0.5, 1.0 and 1.5) ingots. The Mg was first loaded in a graphite crucible which was mounted in a resistance furnace under argon shield. Then, Mg was melted in the furnace at 993 K, followed by adding pure Li, pure Zn and Mg−10Y master-alloys into the Mg melt. The melt was maintained at 993 K for 30 min, and no stirring was used. At last, the melt was poured into a stainless steel mould (*d*60 mm×200 mm). After solidification, a homogenization treatment was carried out at 523 K for 12 h in a vacuum furnace to prepare the ingots for the deformation process. The oxide scale was removed by the numerical control lathe and cut to *d*48 mm prior to deformation. Finally, the LZ83−*x*Y ingots were extruded at 523 K from *d*48 mm to *d*12 mm. The chemical composition of the alloys was measured by atomic absorption spectrometry as shown in Table 1.

Table 1 Chemical composition of experiment alloy (mass fraction, %)

Normal alloys	Nominal composition	Nominal Zn/Y ratio	Actual composition	Actual Zn/Y ratio
I	LZ83	−	Mg−8.2Li−3.2Zn	−
II	LZ83−0.5Y	6:1	Mg−8.3Li−3.1Zn−0.5Y	6.2:1
III	LZ83−1.0Y	3:1	Mg−8.1Li−3.0Zn−1.1Y	2.7:1
IV	LZ83−1.5Y	2:1	Mg−8.3Li−2.9Zn−1.6Y	1.8:1

Before the observation of the microstructure, the specimens were mounted by using the compression-mounting machine, followed by grinding to produce a plane surface with minimal scratches using silicon paper abrasive waterproof. Then, the specimens were polished to obtain a shiny surface. Finally, in order to reveal the details of the microstructures, etching process was done by 2% HNO_3 alcohol etchant solution (volume fraction). Microstructure investigation of Mg−Li alloys was carried out by X-ray diffraction (XRD, D/MAX-IIIC X) and a scanning electron microscope (SEM,TESCAN VEGA2) with energy dispersive spectroscope (EDS). Phase analysis was determined by D/Max2500pc X-ray diffractometer (XRD) using monochromatic Cu K_α radiation. Tensile tests were performed on a CMT−5105 (SANS Materials Analysis Inc., Shenzhen, China) tensile tester with a displacement speed of 0.5 mm/min at room temperature.

3 Result and discussion

3.1Microstructure of as-cast LZ83−*x*Y alloy

The analysis results of the XRD patterns for different alloys are shown in Fig. 1. It is observed that the amount of each phase is dependent on the Zn/Y ratio. The main phases in the microstructure of LZ83 are *β*-Li, *α*-Mg and Mg_7Zn_3. By adding yttrium to LZ83 alloy and obtaining LZ83−0.5Y alloy, the *I*-phase forms for the Zn/Y ratio of 6.2:1. *I*-phase and *W*-phase coexist in LZ83−1.0Y and LZ83−1.5Y alloys because the Zn/Y ratios are 2.7:1 and 1.8:1, respectively. With the increase of the Y content, the diffraction peaks of the *I*-phase become weaker and the amount of the *W*-phase increases. The low intensity of the peaks for *I*-phase and *W*-phase in these two alloys might be due to the low amount of the phases.

Figure 2 shows the SEM micrographs of the alloys. The microstructures of as-cast samples present dual phase, the *β*-Li matrix phases and the irregular *α*-Mg phases, respectively. The phase size of *α*-Mg is not uniformly distributed from ~30 to 150 μm. In Fig. 2(a),

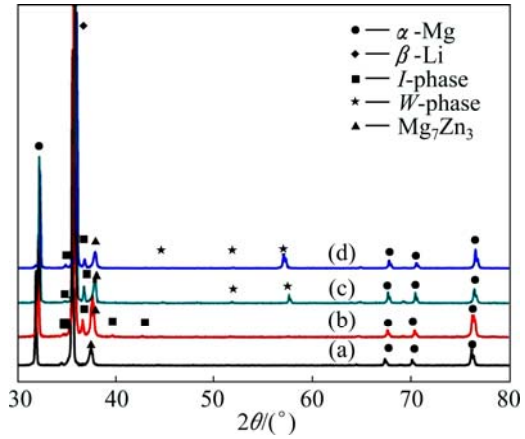

Fig. 1 XRD patterns of alloys: (a) LZ83; (b) LZ83−0.5Y; (c) LZ83−1.0Y; (d) LZ83−1.5Y

there is no apparent precipitated phase observed in the microstructure of LZ83 alloy. It has been reported [5,13] that *I*-phase could form as interdendritic eutectic pockets with *α*-Mg. *I*-phase can also form at the boundary of *α*-Mg phase and *β*-Li matrix. This may suggest that the *I*-phase first nucleates along the grain boundaries and

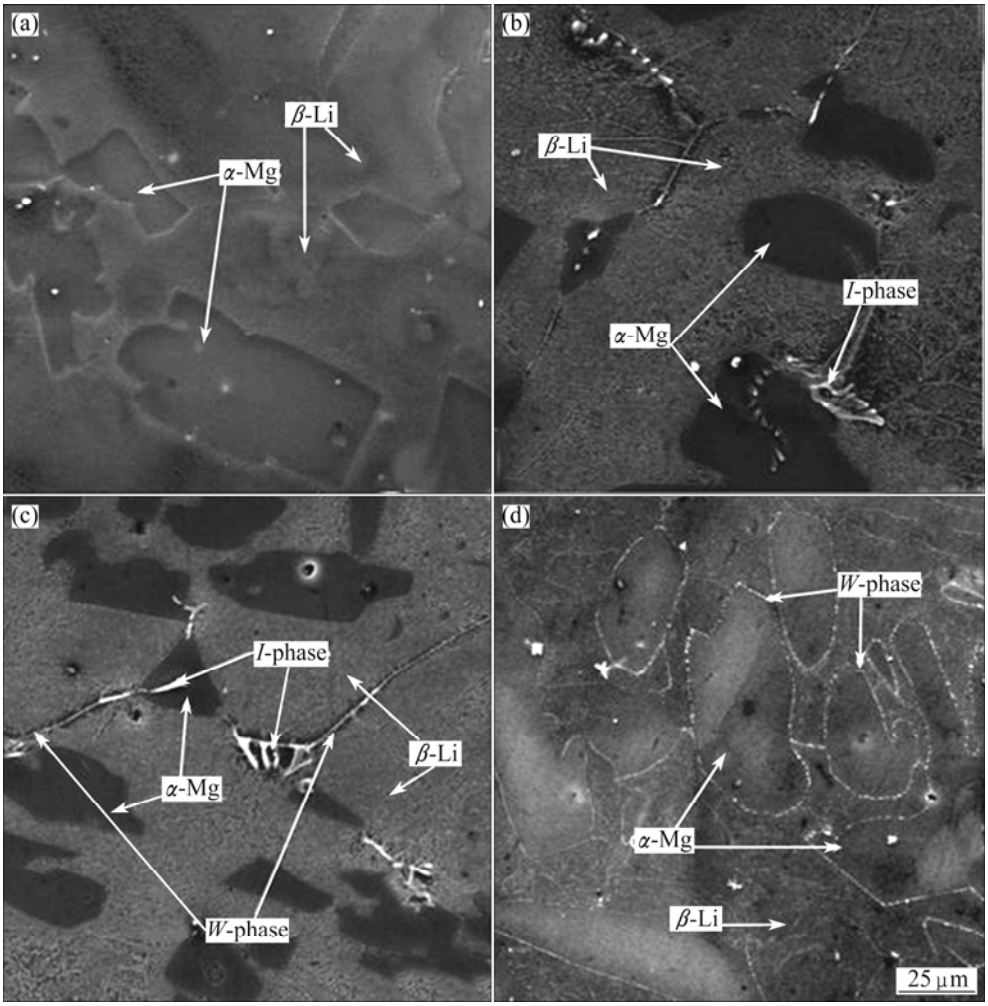

Fig. 2 SEM images of as-cast LZ83−*x*Y alloy: (a) LZ83; (b) LZ83−0.5Y; (c) LZ83−1.0Y; (d) LZ83−1.5Y

then begins to grow into the matrix while the solute diffuses during or after solidification [19]. Therefore, *I*-phase can be determined by considering its morphology and location. In Fig. 2(b), some primary point-like *I*-phases are observed; due to low amounts of Zn and Y, large areas of *I*-phase/*α*-Mg eutectic pockets could not form. It has been observed that *W*-phase can exist at the phase boundaries or the ends of *I*-phase [16,19]. *I*-phase tends to form at the triple junctions of grain boundaries, whereas *W*-phase preferentially forms at the intergranular boundaries, which is an easy way to distinguish *W*-phase from *I*-phase. Some *W*-phases preferentially form at the *α*-Mg/*β*-Li phase interfaces, referring to Fig. 2(c). With the increasing amount of Y, while the Zn/Y ratio is about 1.8:1, more *W*-phase forms but *I*-phase decreases significantly, as observed in Fig. 2(d). It is not easy to find *I*-phase because of its low content. In Fig. 3, the microstructures of *I*-phase and *W*-phase are enlarged and the EDS results show that the white compound is mainly composed of Mg, Zn and Y. This confirms the existence, morphology and location of *I*-phase and *W*-phase.

3.2 Microstructure of extruded LZ83−*x*Y alloy

Figure 4 shows the optical microstructures of extruded LZ83−*x*Y alloys in both extrusion and transverse directions. After severe deformation, the *α*-Mg phase and *β*-Li phase are approximately parallel to the extrusion direction and exhibit elongated structure as shown in Figs. 4(b), (d), (e) and (f). The equiaxial *β*-Li grains are observed in the microstructure which formed via discontinuous dynamic recrystallization (DDRX) process [9]; the average diameters of the grains are about 6.8, 10.0, 7.2 and 7.9 μm by line interception method for LZ83, LZ83−0.5Y, LZ83−1.0Y and LZ 83−1.5Y alloys, respectively. In Figs. 4(d) and (f), the dimension of *α*-Mg phases is not uniform after deformation by continuous dynamic recrystallization (CDRX), because the strong cohesion of *I*-phase can prevent the deformation of *α*-Mg phases and suppress the microstructural evolution [9,23]. During the extrusion process, the as-cast brittle *I*-phase and *W*-phase formed at the grain boundary were broken, providing the distribution of small particles with nanoscale size in the matrix as shown in Fig. 5. The small *I*-phase/*α*-Mg eutectic pockets in the as-cast alloy

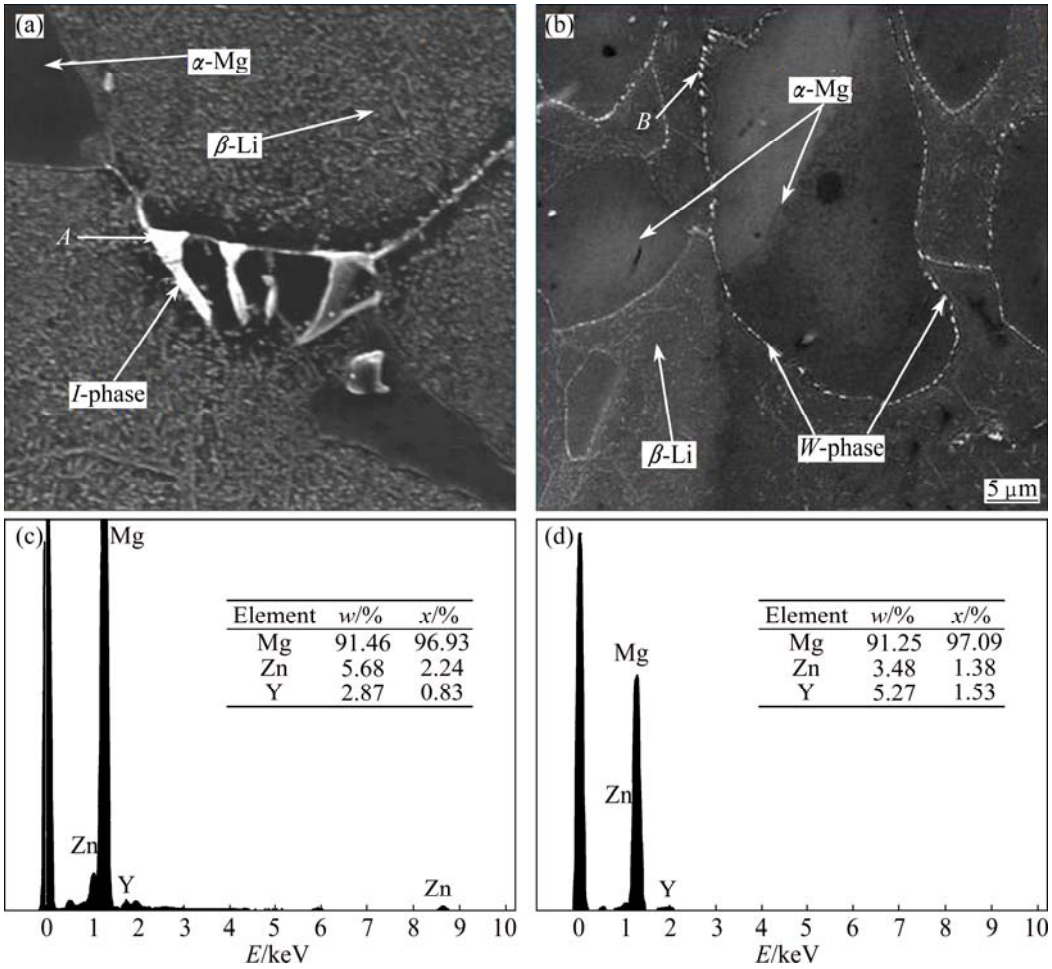

Fig. 3 SEM images (a, b) and EDS results (c, d) of *I*-phase and *W*-phase: (a, c) *I*-phase in LZ83−Y alloy; (b, d) *W*-phase in LZ83−1.5Y alloy

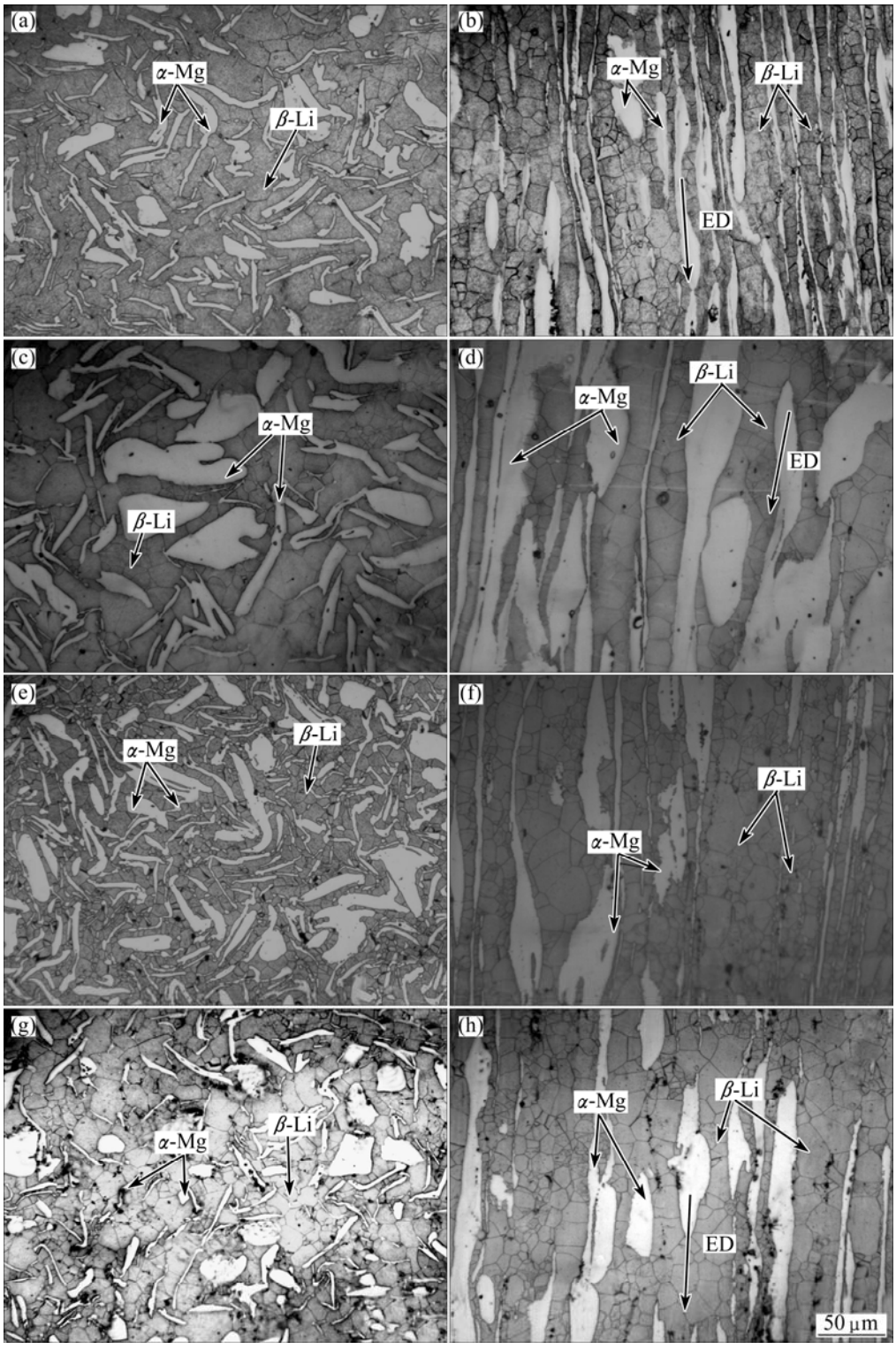

Fig. 4 Optical images of extruded LZ83−*x*Y alloys in cross section (a, c, e, g) and longitudinal section (b, d, f, h): (a, b) LZ83; (c, d) LZ83−0.5Y; (e, f) LZ83−1.0Y; (g, h) LZ83−1.5Y

were broken and more particles were distributed in *β*-Li phase during the extrusion since *β*-Li phase was softer compared with the *α*-Mg phase [10] as shown in Fig. 5(b). With the increasing amount of Y in LZ83−1.5Y alloy, more *W*-phase particles were dispersed in *β*-Li phase and the boundaries between *α*-Mg and *β*-Li phases.

3.3 Room temperature mechanical properties

The stress−strain curves of LZ83−*x*Y alloys at room temperature are shown in Fig. 6. The ductility generally decreases as the strength increases and the apparent

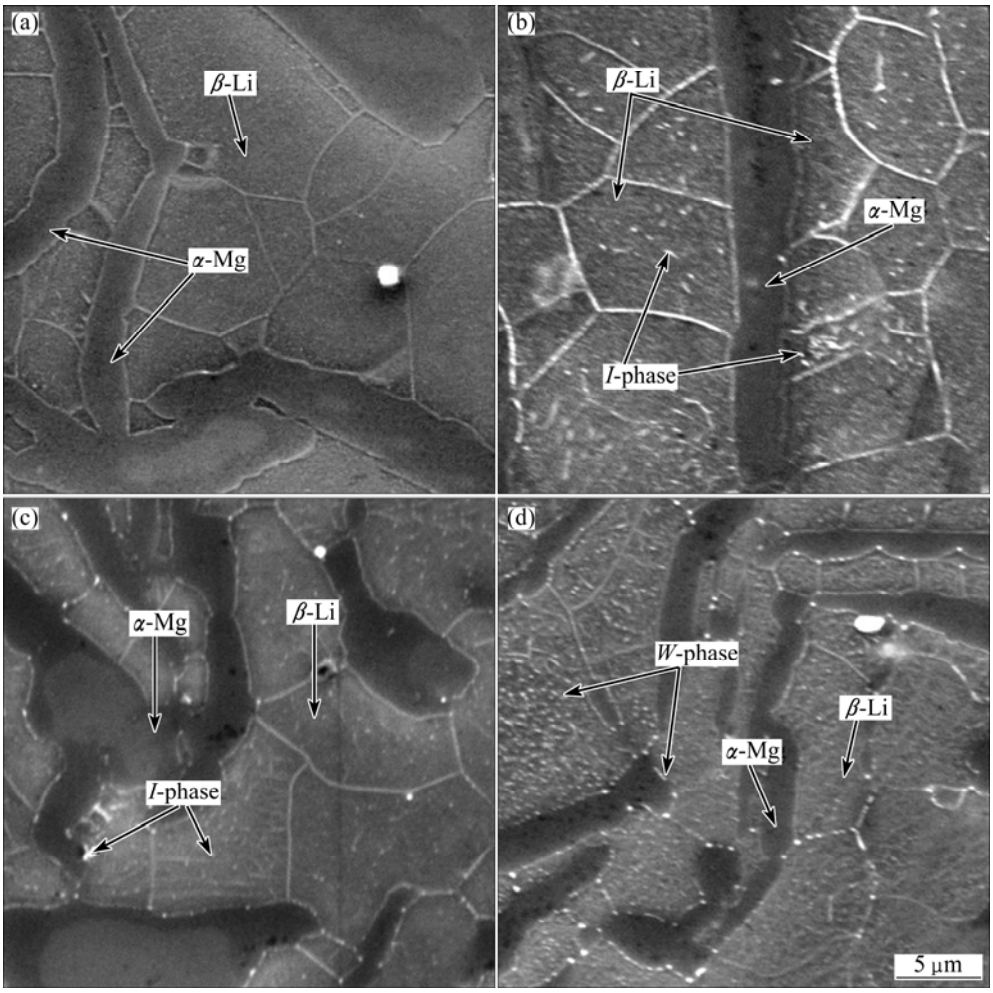

Fig. 5 SEM images of extruded LZ83−*x*Y alloy: (a) LZ83; (b) LZ83−0.5Y; (c) LZ83−1.0Y; (d) LZ83−1.5Y

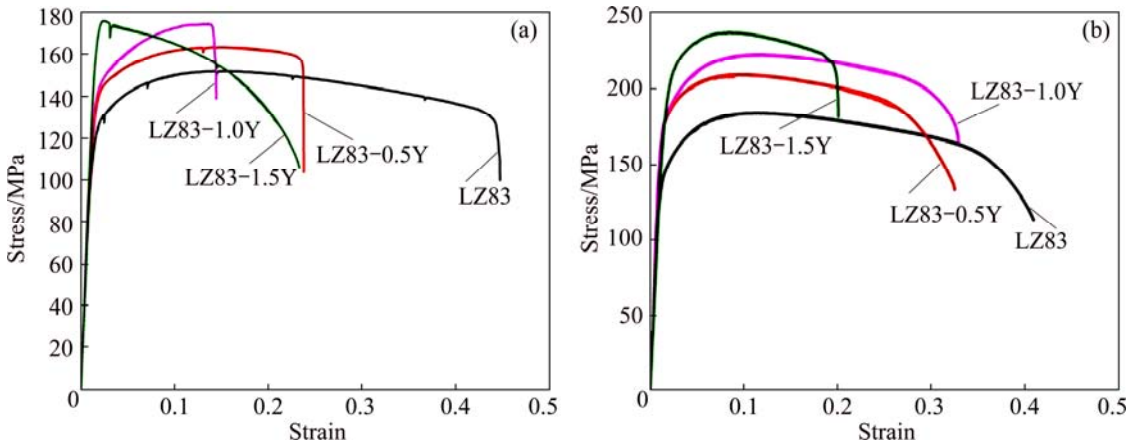

Fig. 6 Stress−strain curves of LZ83−*x*Y alloys at room temperature: (a) As-cast alloy; (b) Extruded alloy

stress drops sharply due to necking near the final fracture strain. Referring to Fig. 6(a), the elongation to failure (δ) of as-cast LZ83 alloy is about 44% and the ultimate tensile strength (σ_b) is 151 MPa; while for the as-cast Mg−8Li−3Al alloy, the strength is 142 MPa and the elongation is only 7% [10]. The mechanical properties are in good agreement with the conclusions of the previous study that the addition of Zn into Mg alloy has positive effects on the ductility [6]. It can be seen that adding Y can effectively improve the strength in both as-cast and extruded alloys. This may be contributed to formation of new compounds. Generally, elongation is low for alloys containing a large amount or large size of intermetallic particles since geometrically necessary

dislocations are formed in the region surrounding the hard particle, leading to decohesion from the matrix [24]. But the stability of *I*-phase can provide a large elongation with no void opening at the interface between the quasicrystalline particle and the α-Mg matrix in as-cast alloy [17,18]. As shown in Table 2, due to the pinning effect of *I*-phase particles in as-cast LZ83−0.5Y alloy, the ultimate tensile strength is about 163 MPa and the elongation is 23%, higher than those of Mg−8Li−3Al−1.0Y (LAY831, σ_b is 145.77 MPa, ε is 12%) [10]. A continuous stress−strain curve with no obvious yield point elongation in the as-cast LZ83−1.0Y alloys is observed. The *I*-phase and *W*-phase with finer net-like microstructure distributed at the grain boundaries can effectively retard the dislocation movement. Consequently, the strength of alloys can be improved with a certain amount of *W*-phase. The LZ83−1.5Y alloy presents a moderate combination in mechanical properties; σ_b reaches 175 MPa and ε is 23%. But after yielding, strength softening occurs, which is also observed for LZ83 alloy. So, the strengthening effect of *W*-phase is lower than *I*-phase in the as-cast alloys as observed in the previous studies [14,19,24]. *I*-phase-reinforced alloys (LZ83−0.5Y and LZ83−1.0Y) exhibit strain hardening all through the test. In the tensile test, a large number of quasicrystalline particles in the Mg−Li alloys can effectively prohibit microstructural evolution of the α-Mg phase during deformation [14]. When an alloy possesses *I*-phase as a second phase, it is stable against coarsening due to the low interfacial energy of the quasicrystals, providing improved bonding properties at *I*-phase/matrix interface [19]. So, the stable quasicrystalline particle/matrix interface provides a large elongation and continuous strain hardening with no void opening at the interface between the quasicrystalline particle and the matrix.

Referring to Fig. 6(b) and Table 2, the mechanical properties of LZ83−*x*Y alloys are raised substantially after extrusion due to grain boundary strengthening and dispersion strengthening of finely dispersed *I*-phase and *W*-phase particles [18]. The LZ83−1.5Y alloy possesses excellent σ_b (238 MPa), compared with as-extruded LAY831 (σ_b is 209.88 MPa) and LA83−1Ce−1Ca (σ_b is about 228 MPa) [10,25]. It can be seen that the *I*-phase improves the strength and the *W*-phase does not deteriorate the mechanical properties. It was reported that the α-Mg/*I*-phase eutectic pockets can supply the rigid bonding during the deformation in both as-cast and extruded alloys, because the *I*-phase always exists in α-Mg matrix such as in Mg−Zn−Y or Mg−Zn−Y−Zr alloys [19], so the *I*-phase can enhance the strength of Mg−Zn−Y alloys. During the extrusion of LZ83−*x*Y alloys, the original morphology and structure of *I*-phase and *W*-phase were broken from micron-size to nanoscale size and most particles were extruded into the soft β-Li. The cohesion effect of *I*-phase in the as-cast alloy converts to dispersion strengthening in the extruded LZ83−0.5Y and LZ83−1.0Y alloys. The strength of extruded alloys depends on the fraction of *I*-phase and *W*-phase particles, so the strengthening effect of *W*-phase is more than that of *I*-phase in the extruded LZ83−*x*Y alloys. This phenomenon is different from the previous analysis. The primary cause is that the existence zone of *I*-phase and *W*-phase changes from α-Mg phase into β-Li phase. So, the *I*-phase loses its advantage of strengthening and the strengthening effect of *W*-phase is more obvious because of its higher volume fraction.

Table 2 Mechanical properties of LZ83−*x*Y alloys

Alloy	As-cast			As-extruded		
	δ/%	σ_s/MPa	σ_b/MPa	δ/%	σ_s/MPa	σ_b/MPa
LZ83	44	106	151	40	137	183
LZ83−0.5Y	23	119	163	32	176	209
LZ83−1.0Y	14	131	174	32	177	222
LZ83−1.5Y	23	164	175	20	192	238

4 Conclusions

1) The microstructures of LZ83−*x*Y alloys are mainly comprised of BCC β-Li, HCP α-Mg and Mg_7Zn_3 phases and the fraction volumes of *I*-phase and *W*-phase are dependent on Zn/Y ratio.

2) In as-cast LZ83−*x*Y alloys, *I*-phase is mainly formed in α-Mg phase and α/β phase boundary with the form of *I*-phase/α-Mg eutectic pockets. The *W*-phase mainly precipitates continuously along α/β phase boundary. The as-cast LZ83 alloy exhibits high plasticity with a maximum elongation of 44% in tensile test at room temperature. *I*-phase can enhance the strength in as-cast LZ83−0.5Y and LZ83−1.0Y alloys, *W*-phase has no obvious strengthening effect on LZ83−1.5Y alloy.

3) In the as-extruded LZ83−*x*Y alloys, the *I*-phase and *W*-phase are broken into nanoscale particles and mainly disperse in β-Li matrix. The LZ83−1.5Y alloy possesses the excellent mechanical properties due to dispersion strengthening of *W*-phase, the σ_b is 238 MPa and δ is 20%.

References

[1] YAN Yong-de, ZHANG Mi-lin, XUE Yun, HAN Wei, CAO Dian-xue, JING Xiao-yan, HE Li-yi, YUAN Yi. Electrochemical formation of Mg−Li−Ca alloys by codeposition of Mg, Li and Ca from LiCl−KCl−$MgCl_2$−$CaCl_2$ melts [J]. Phys Chem Chem Phys, 2009, 11: 6148−6155.

[2] ZENG Ying, JIANG Bin, HUANG De-hui, DAI Jia-hong, PAN Fu-sheng. Effect of Ca addition on grain refinement of Mg−9Li−1Al alloy [J]. Journal of Magnesium and Alloys, 2013, 1(4): 297−302.

[3] JIANG Bin, ZENG Ying, ZHANG Ming-xing, YIN Heng-mei, YANG Qing-shan, PAN Fu-sheng. Effects of Sn on microstructure of as-cast and as-extruded Mg−9Li alloys [J]. Transactions of Nonferrous Metals Society of China, 2013, 23: 904−908.
[4] SONG Guang-ling. Corrosion of magnesium alloys [M]. England: Woodhead Publishing Ltd, 2011: 67−72.
[5] Properties and selection: Nonferrous alloys and special-purpose materials [M]. Amercian: ASM International, 1993: 265−289.
[6] WU Rui-zhi, QU Zhi-kui, ZHANG Mi-lin. Reviews on the influence of alloying elements on the microstructure and mechanical properties of Mg−Li base alloys [J]. Reviews on Advanced Materials Science, 2010, 24: 35−43.
[7] JIANG Bin, YIN Heng-mei, YANG Qing-shan, LI Rui-hong, PAN Fu-sheng. Effect of stannum addition on microstructure of as-cast and as-extruded Mg−5Li alloys [J]. Transactions of Nonferrous Metals Society of China, 2011, 21(11): 2378−2383.
[8] YAN Hong, CHEN Rong-shi, HAN En-hou. Microstructures and mechanical properties of cold rolled Mg−8Li and Mg−8Li−2Al−2RE alloys [J]. Transactions of Nonferrous Metals Society of China, 2010, 20(S2): s550−s554.
[9] YANG Yan, PENG Xiao-dong, WEN Hai-ming, ZHENG Bao-long, ZHOU Yi-Zheng, XIE Wei-dong, LAVERNIA E J. Influence of extrusion on the microstructure and mechanical behavior of Mg−9Li−3Al−*x*Sr alloys [J]. Metall Mater Trans A, 2013, 44: 1101−1113.
[10] WU Rui-zhi, QU Zhi-kui, ZHANG Mi-lin. Effects of the addition of Y in Mg−8Li−(1,3)Al alloy [J]. Materials Science and Engineering A, 2009, 516: 96−99.
[11] SONG G S, STAIGER M, KRAL M. Some new characteristics of the strengthening phase in *β*-phase magnesium–lithium alloys containing aluminum and beryllium [J]. Materials Science and Engineering A, 2004, 371: 371−376.
[12] WANG P C, LIN H C, LIN K M, YEH M T, LIN C Y. A study of aging treatment on the Mg−10Li−0.5Zn alloy [J]. Materials Transactions, 2009, 50: 2259−2263.
[13] CHANG H W, QIU D, TAYLOR J A, EASTON M A, ZHANG M X. The role of Al_2Y in grain refinement in Mg−Al−Y alloy system [J]. Journal of Magnesium and Alloys, 2013, 1(2): 115−121.
[14] XU Dao-kui, TANG Wei-neng, LIU Lu, XU Yong-bo, HAN En-hou. Effect of Y concentration on the microstructure and mechanical properties of as-cast Mg−Zn−Y−Zr alloys [J]. Journal of Alloys and Compounds, 2007, 432: 129−134.
[15] LUO Zhi-ping. High-resolution electron microscopy on the X-Mg_{12}ZnY phase in a high strength Mg−Zn−Zr−Y magnesium alloy [J]. Journal of Materials Science Letters, 2000, 19: 813−815.
[16] XU Dao-kui, LIU Lu, XU Yong-bo, HAN En-hou. The strengthening effect of icosahedral phase on as-extruded Mg−Li alloys [J]. Scripta Materialia, 2007, 57: 285−288.
[17] XU Dao-kui, LIU Lu, XU Yong-bo, HAN En-hou. The influence of element Y on the mechanical properties of the as-extruded Mg−Zn−Y−Zr alloys [J]. Journal of Alloys and Compounds, 2006, 426: 155−161.
[18] LEE J Y, KIM D H, LIM H K, KIM D H. Effects of Zn/Y ratio on microstructure and mechanical properties of Mg−Zn−Y alloys [J]. Materials Letters, 2005, 59: 3801−3805.
[19] XU Dao-kui, HAN En-hou. Effects of icosahedral phase formation on the microstructure and mechanical improvement of Mg alloys: A review [J]. Progress in Natural Science: Materials International, 2012, 22: 364−385.
[20] XU Dao-kui, TANG Wei-neng, LIU Lu, XU Yong-bo, HAN En-hou. Effect of *W*-phase on the mechanical properties of as-cast Mg−Zn−Y−Zr alloys [J]. Journal of Alloys and Compounds, 2008, 461: 248−252.
[21] YANG Wen-peng, GUO Xue-feng. High strength magnesium alloy with *α*-Mg and *W*-phase processed by hot extrusion [J]. Transactions of Nonferrous Metals Society of China, 2011, 21(11): 2358−2364.
[22] ZHENG M Y, XU S W, WU K, KAMADO S, KOJIMA Y. Superplasticity of Mg−Zn−Y alloy containing quasicrystal phase processed by equal channel angular pressing [J]. Materials Letters, 2007, 61: 4406−4408.
[23] BAE D H, KIM S H, KIM D H, KIM W T. Deformation behavior of Mg−Zn−Y alloys reinforced by icosahedral quasicrystalline particles [J]. Acta Materialia, 2002, 50: 2343−2356.
[24] BAE D H, LEE M H, KIM K T, KIM W T, KIM D H. Application of quasicrystalline particles as a strengthening phase in Mg−Zn−Y alloys [J]. Journal of Alloys and Compounds, 2002, 342: 445−450.
[25] CHENG Li-ren, CAO Zhan-yi, WU Rui-zhi, ZHANG Mi-lin, JIANG Dong-mei. Microstructure and mechanical properties of the as-cast and extruded Mg−(6−11)Li−3Al−Ce−Ca alloys [J]. Materials Transactions, 2010, 51: 1526−1530.

I 相和 *W* 相对 Mg−8Li−3Zn 镁合金显微组织和力学性能的影响

魏国兵[1]，彭晓东[1,2]，张 宝[1]，Amir HADADZADEH[3]，许天才[1]，谢卫东[1,2]

1. 重庆大学 材料科学与工程学院，重庆 400044；
2. 重庆大学 国家镁合金材料工程技术研究中心，重庆 400044；
3. Department of Mechanical and Mechatronics Engineering, University of Waterloo, Waterloo ON N2L 3G1, Canada

摘 要：通过 XRD、OM、SEM 和 EDS 研究 *I* 相和 *W* 相对 LZ83−*x*Y 镁合金显微组织和力学性能的影响。结果表明：LZ83−*x*Y 合金中 *I* 相和 *W* 相的含量变化与 Zn/Y 质量比有关。*I*/*α*-Mg 共晶包的结合力可以增强铸态 LZ83−0.5Y 和 LZ83−1.0Y 合金的强度，同时 *W* 相对 LZ83−1.5Y 镁合金没有明显的强化效果。在挤压态合金中，*I* 相和 *W* 相被挤压成纳米颗粒弥散在 *β*-Li 基体中。由于 *W* 相的体积分数较高，其弥散强化效果更为明显。挤压态 LZ83−1.5Y 镁合金的极限抗拉强度达到 238 MPa，伸长率为 20%。

关键词：Mg−8Li−3Zn 合金；*I* 相；*W* 相；力学性能；铸态组织

(Edited by Xiang-qun LI)